Electronic Supplementary Information

Rational strategy to develop boron nitride quantum dots based molecular logic gate and fluorescent assay of alkaline phosphatase activity

Yaqian Han[a], *Yusheng Niu*[b], *Mengli Liu*[a], *Fushang Niu*[a] *and Yuanhong Xu*[a,b,]*

[a] Institute for Graphene Applied Technology Innovation, College of Materials Science and Engineering, Qingdao University, Qingdao 266071, China

[b] College of Life Sciences, Qingdao University, Qingdao 266003, China

Yaqian Han and Yusheng Niu contributed equally to this work.

Experimental Section

Materials: Boron nitride (98.5%, AR) was obtained from Shangdong Laiyang Economic and Technological Development Zone Chemical Plant (Shandong, China). Alkaline phosphatase (ALP) and pyrophosphate anions (PPi) were purchased from Sigma-Aldrich (Steinheim, Germany).Silver nitrate, mercuric nitrate were purchased from Aladdin Reagent Co., Ltd (Shanghai, China). Aluminum chloride, sodium sulfate, potassium chloride, chromium acetate, ferric chloride, copper chloride, cobalt chloride, ferrous chloride, magnesium chloride, lead acetate, manganese chloride, zinc chloride, and nickel nitrate were obtained from Tianjin Reagent Co., Ltd (Tianjin, China). All other chemicals were of at least analytical grade and used as received without further purification. The water used throughout the experiments was purified through a Milli-Q water system.

Preparation of BNQDs: Typically, 0.1 g BN powder and 15 mL of ethanol were added in a beaker (20 mL) and BN powder was exfoliated into nanosheets after sonication for 3 h by ultrasonic cell crusher with an output power of 500 W. The solution was then transferred to a Teflon-lined stainless steel autoclave with the filling factor of 2/3 and heated in vacuum drying oven at 180 ℃ for 10 h. Afterward, the reaction mixture was cooled down naturally to room temperature. The as-prepared

BNQDs scattered the supernatant were collected by centrifuging the resulted suspensions at 12000 rpm for 10 min. The supernatant of BNQDs was used for the following characterizations.

Characterizations: The FL measurements were performed on an Edinburgh instruments spectrofluorometer FS5 (Edinburgh, U. K.). The ultraviolet-visible (UV-Vis) absorption spectra was obtained from a Mapada UV-1800PC spectrophotometer (Shanghai, China). Fourier transform infrared (FTIR) data were measured on Nicolet Nexus 5700 (Thermo Electron Corporation, USA). X-ray photoelectron spectroscopy (XPS) data were obtained on an ESCALab220i-XL electron spectrometer (VG Scientific, West Sussex, U. K.) using 300 W Al Kα radiation. Atomic force microscopy (AFM) images were collected from SPI3800N microscope (Seiko Instruments Inc., Japan). Transmission electron microscopy (TEM) was carried out by a JEOL Ltd JEM-2010 transmission electron microscope (JEOL Ltd., Japan).

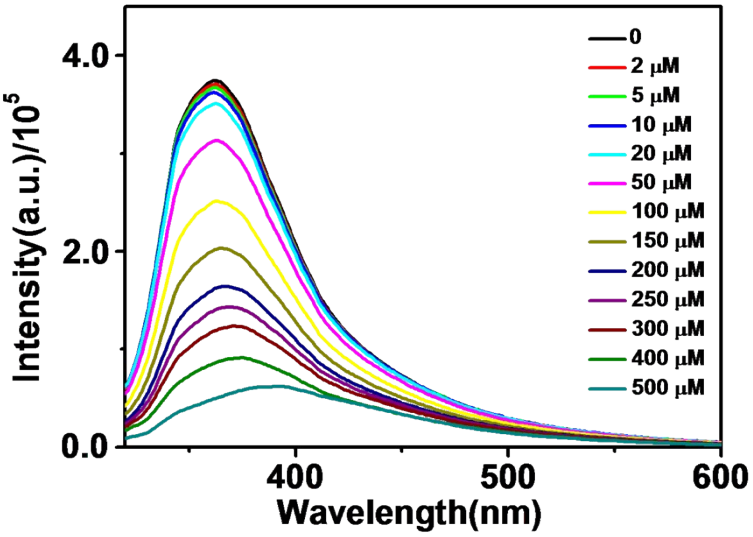

Fig. S1. FL intensity of BNQDs excited at 318 nm in the presence of different concentrations of Fe^{3+} from 2 to 500μM.

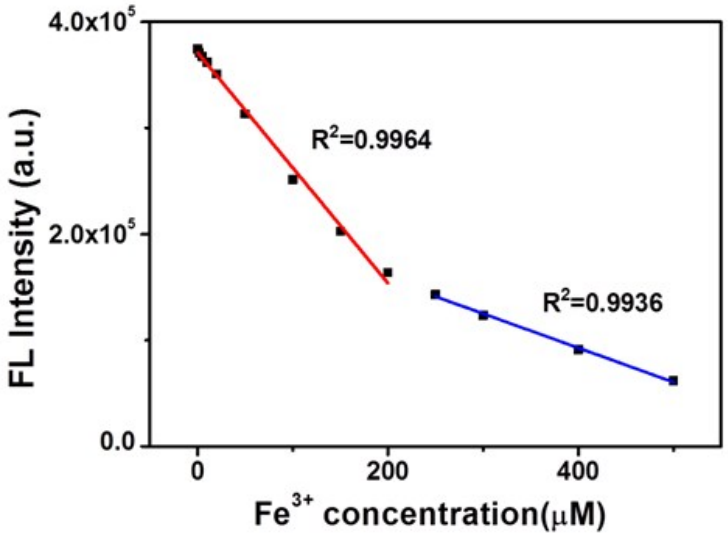

Fig. S2. The corresponding linear relationship of FL intensity $(I-I_0)/I_0$ and the concentration of Fe^{3+}.

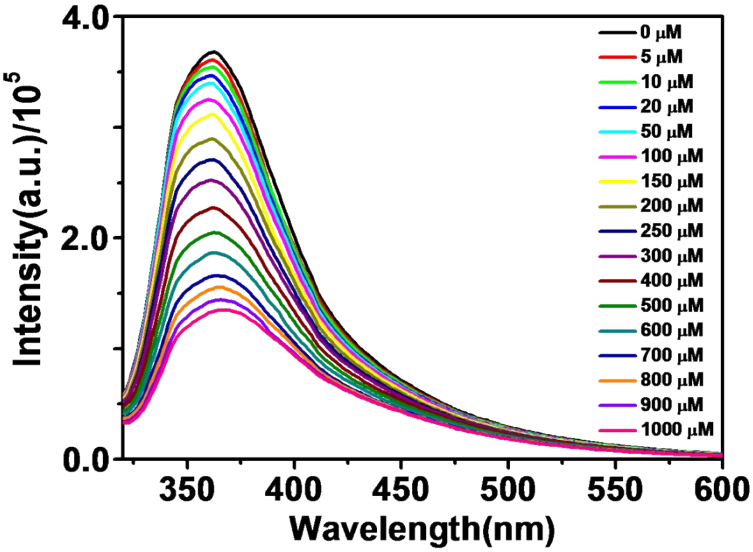

Fig. S3. FL intensity of BNQDs excited at 318 nm in the presence of different concentrations of Cu^{2+} from 5 to 1000μM.

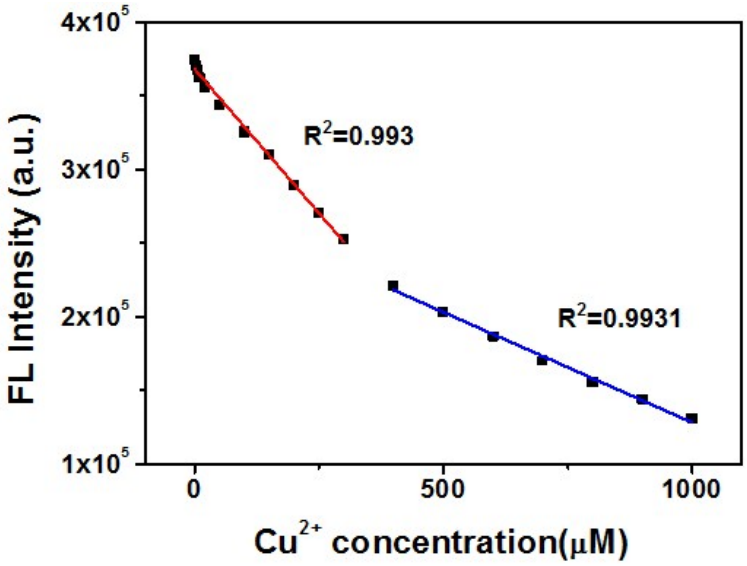

Fig. S4. The corresponding linear relationship of FL intensity $(I-I_0)/I_0$ and the concentration of Cu^{2+}.

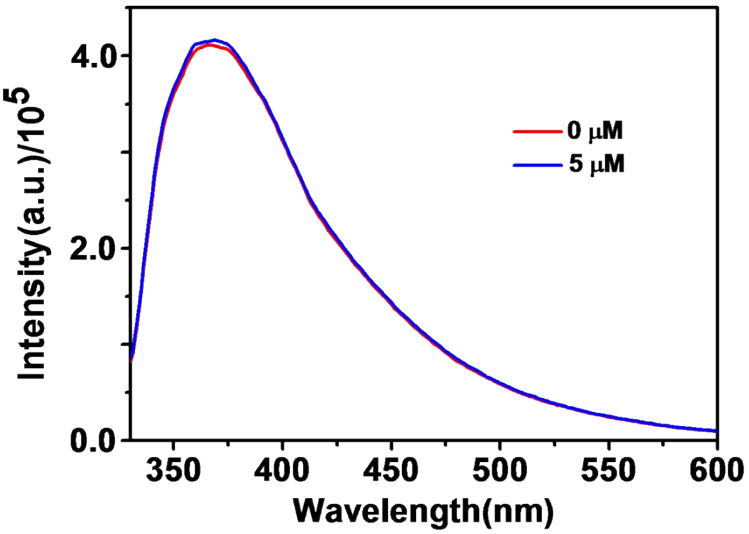

Fig. S5. The changes of FL spectra of BNQDs-Fe^{3+} (5μM) mixture with increasing concentrations of PPi under excitation wavelength of 318 nm.

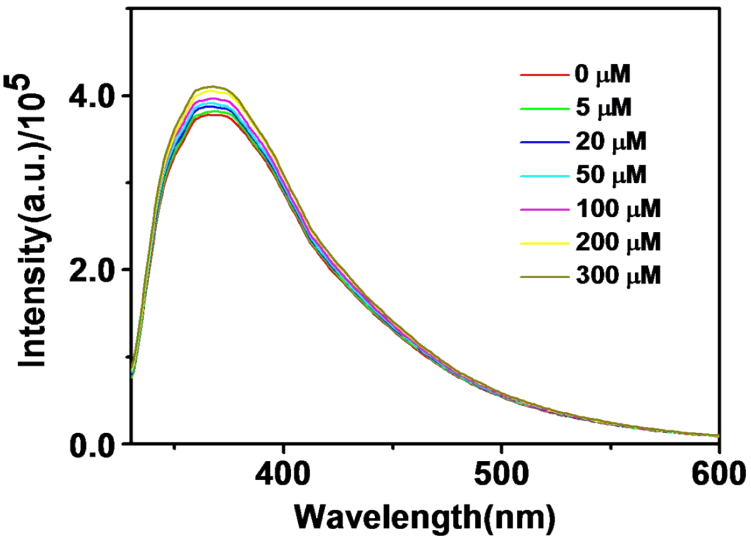

Fig. S6. The changes of FL spectra of BNQDs-Fe^{3+} (20μM) mixture with increasing concentrations of PPi under excitation wavelength of 318 nm.

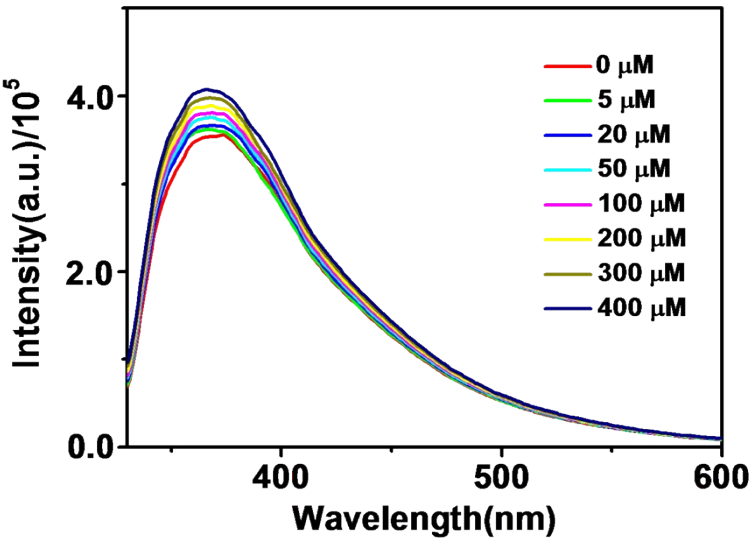

Fig. S7. The changes of FL spectra of BNQDs-Fe^{3+} (50μM) mixture with increasing concentrations of PPi under excitation wavelength of 318 nm.

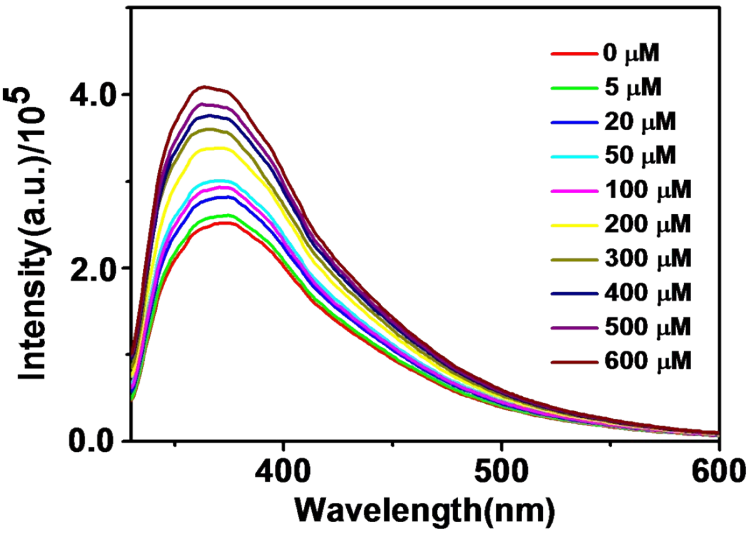

Fig. S8. The changes of FL spectra of BNQDs-Fe^{3+} (100μM) mixture with increasing concentrations of PPi under excitation wavelength of 318 nm.

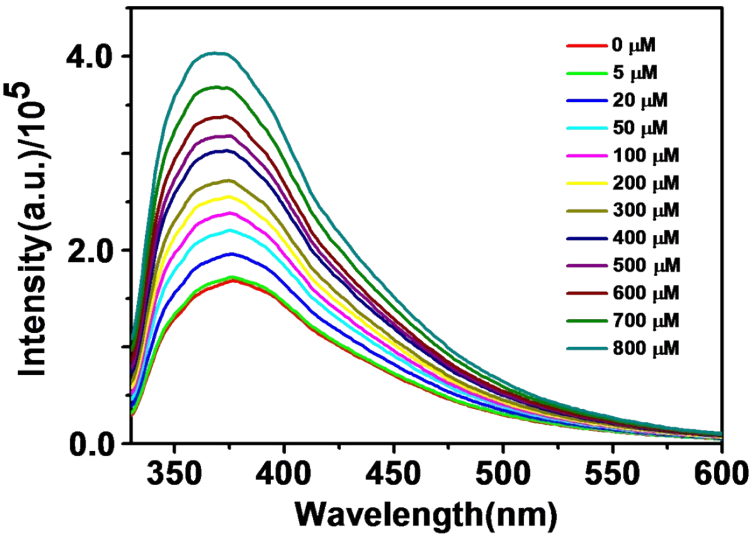

Fig. S9. The changes of FL spectra of BNQDs-Fe^{3+} (200μM) mixture with increasing concentrations of PPi under excitation wavelength of 318 nm.

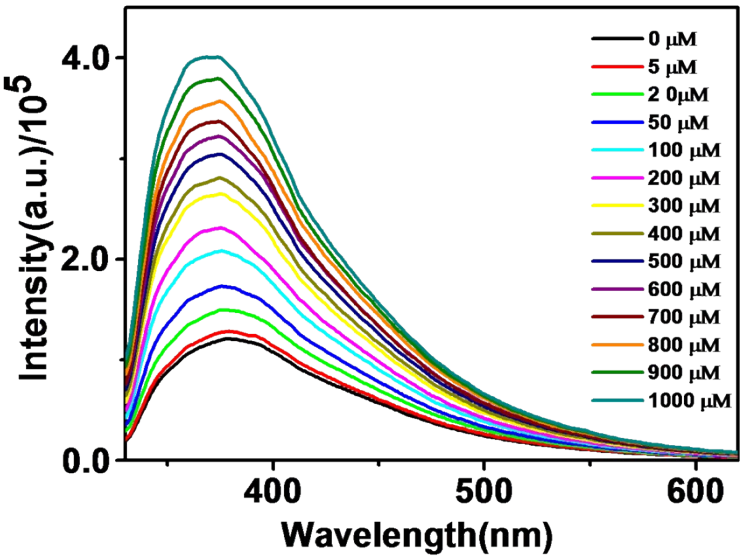

Fig. S10. The changes of FL spectra of BNQDs-Fe^{3+} (300μM) mixture with increasing concentrations of PPi under excitation wavelength of 318 nm.

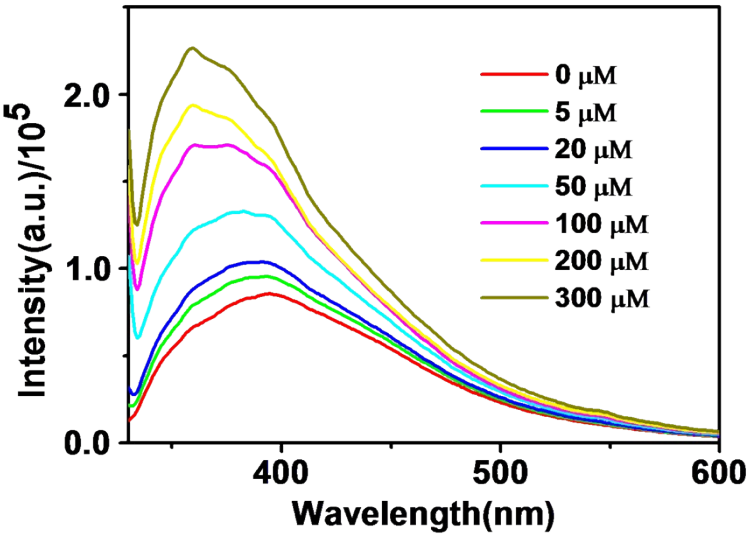

Fig. S11. The changes of FL spectra of BNQDs-Fe^{3+} (400μM) mixture with increasing concentrations of PPi under excitation wavelength of 318 nm.

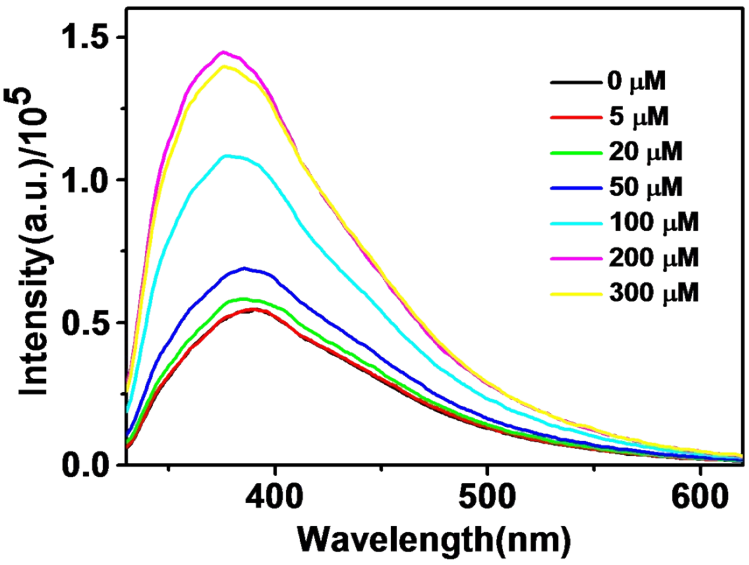

Fig. S12. The changes of FL spectra of BNQDs-Fe^{3+} (500μM) mixture with increasing concentrations of PPi under excitation wavelength of 318 nm.

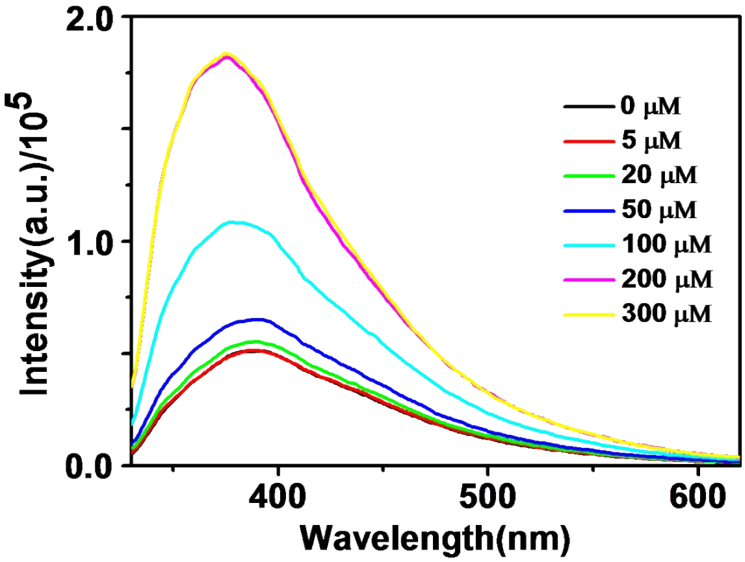

Fig. S13. The changes of FL spectra of BNQDs-Fe^{3+} (600μM) mixture with increasing concentrations of PPi under excitation wavelength of 318 nm.

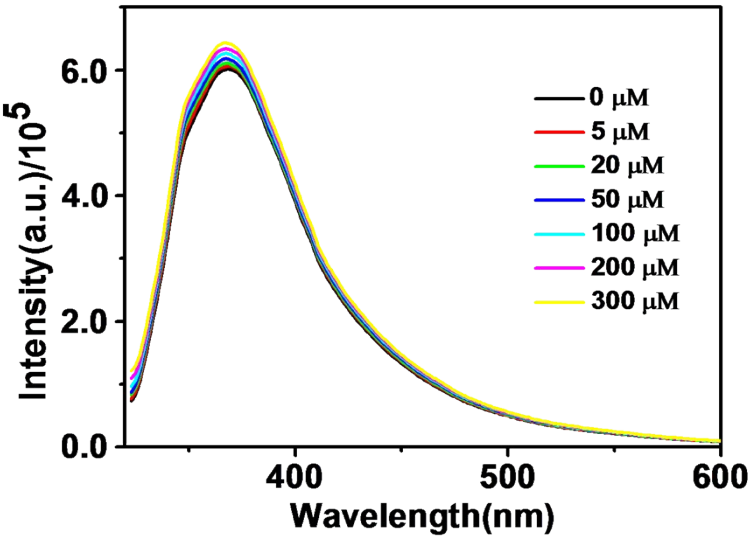

Fig. S14. The changes of FL spectra of BNQDs-Cu^{2+} (5μM) mixture with increasing concentrations of PPi under excitation wavelength of 318 nm.

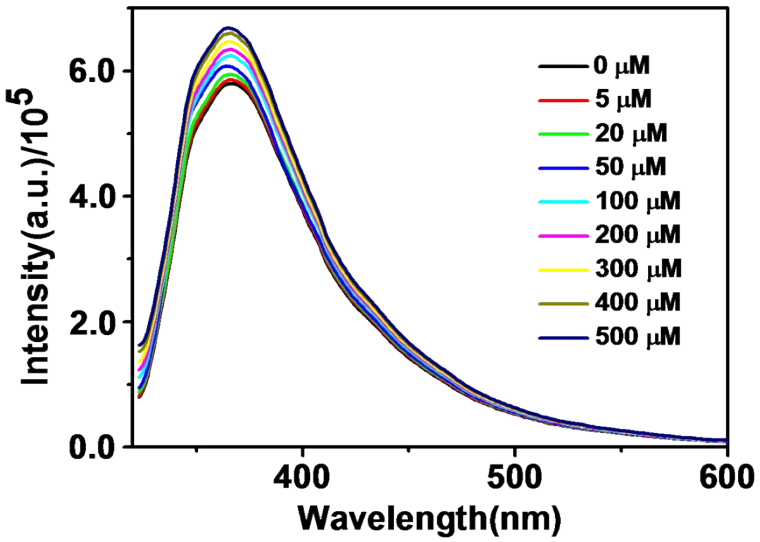

Fig. S15. The changes of FL spectra of BNQDs-Cu^{2+} (20μM) mixture with increasing concentrations of PPi under excitation wavelength of 318 nm.

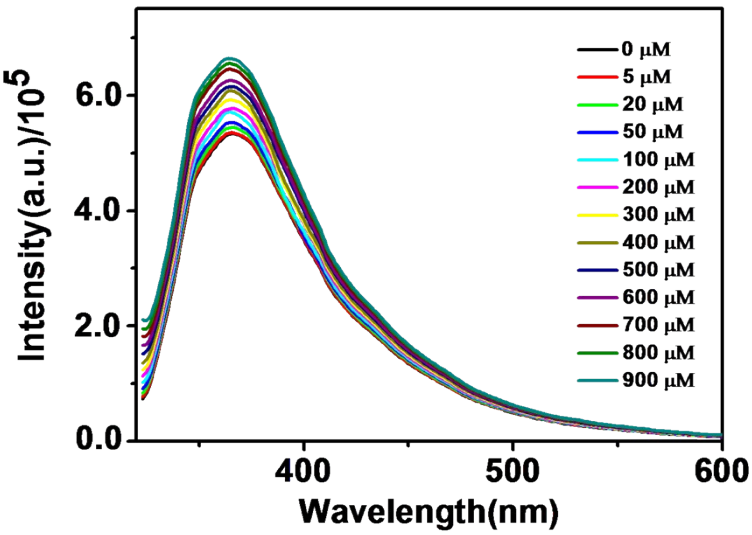

Fig. S16. The changes of FL spectra of BNQDs-Cu^{2+} (50μM) mixture with increasing concentrations of PPi under excitation wavelength of 318 nm.

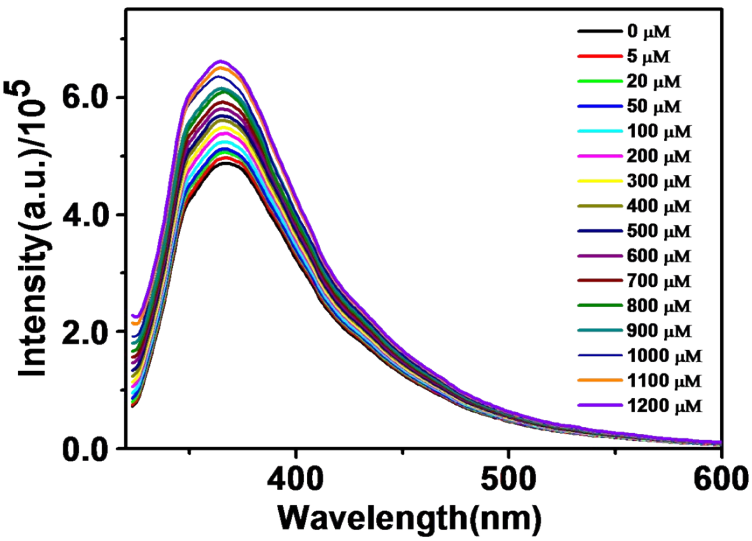

Fig. S17. The changes of FL spectra of BNQDs-Cu^{2+} (100μM) mixture with increasing concentrations of PPi under excitation wavelength of 318 nm.

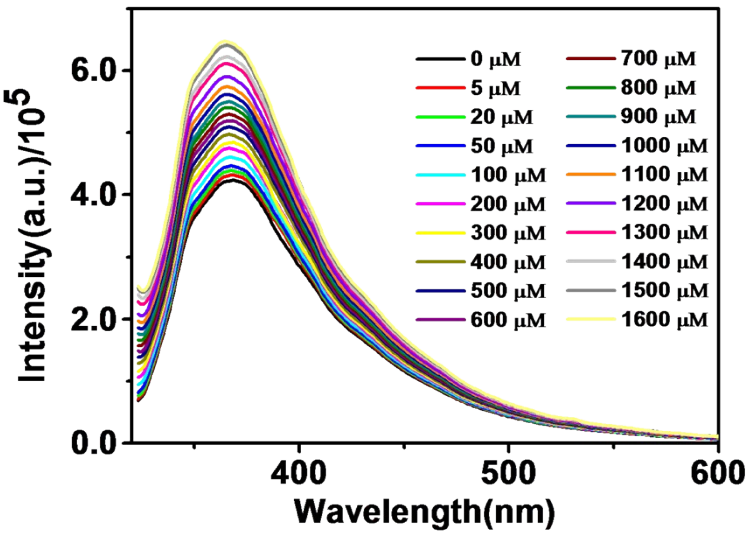

Fig. S18. The changes of FL spectra of BNQDs-Cu^{2+} (200μM) mixture with increasing concentrations of PPi under excitation wavelength of 318 nm.

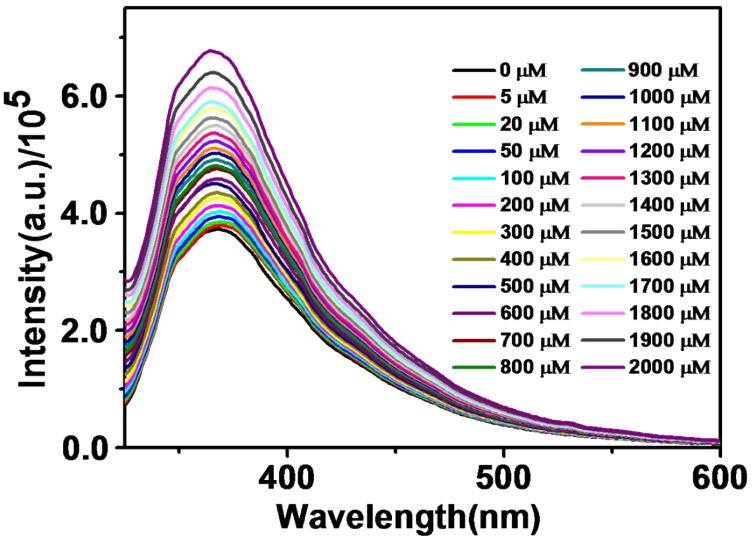

Fig. S19. The changes of FL spectra of BNQDs-Cu^{2+} (300μM) mixture with increasing concentrations of PPi under excitation wavelength of 318 nm.

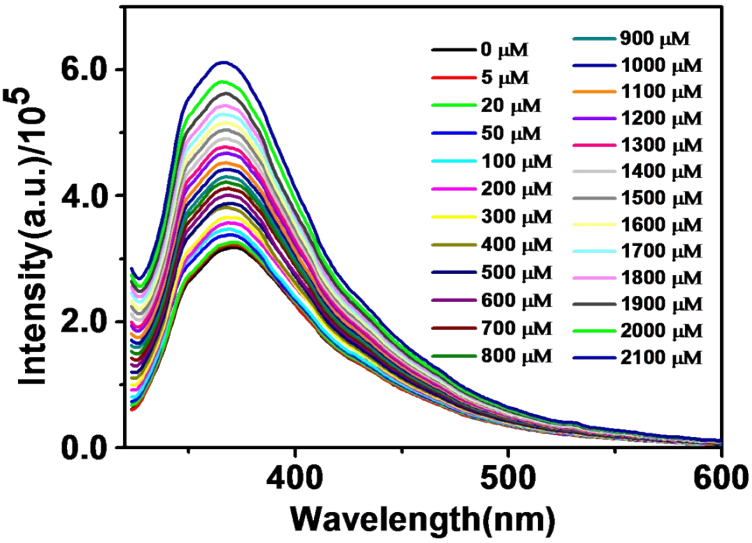

Fig. S20. The changes of FL spectra of BNQDs-Cu^{2+} (400μM) mixture with increasing concentrations of PPi under excitation wavelength of 318 nm.

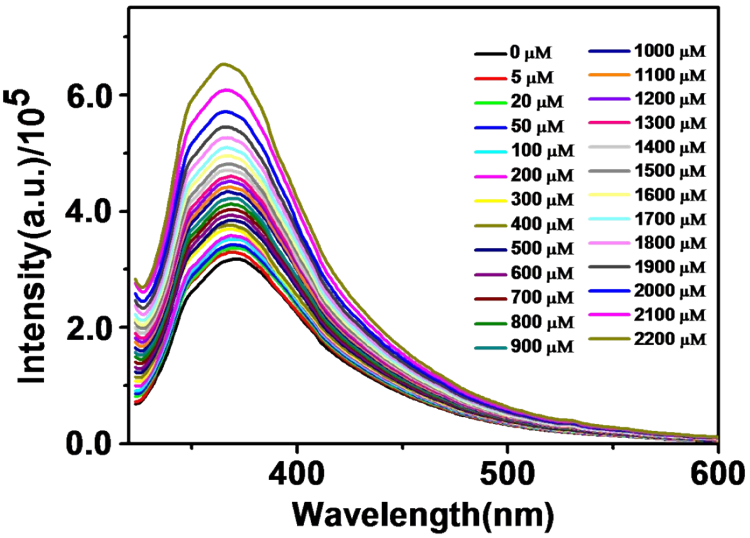

Fig. S21. The changes of FL spectra of BNQDs-Cu^{2+} (500μM) mixture with increasing concentrations of PPi under excitation wavelength of 318 nm.

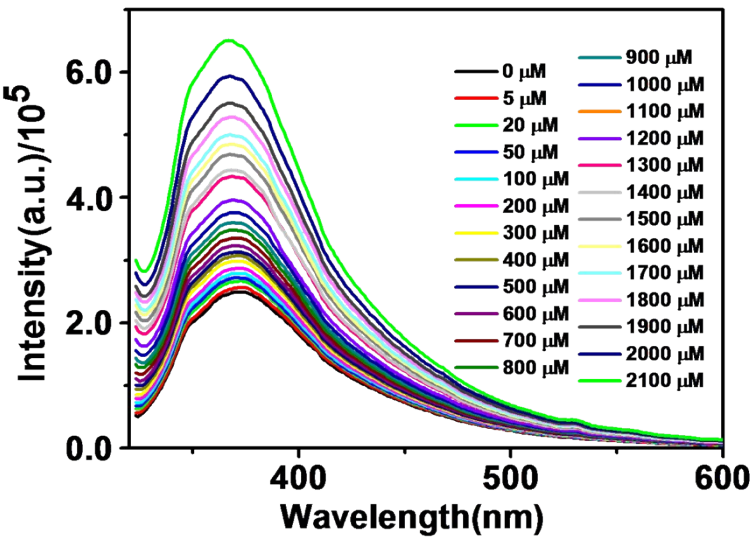

Fig. S22. The changes of FL spectra of BNQDs-Cu^{2+} (600μM) mixture with increasing concentrations of PPi under excitation wavelength of 318 nm.

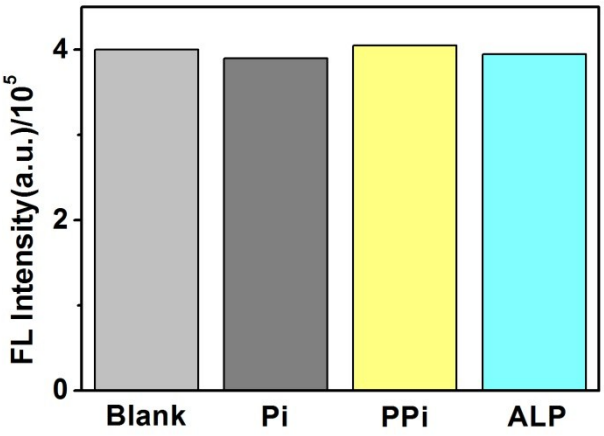

Fig. S23. FL intensity of mixture by separate addition of Pi, PPi, ALP to BNQDs solutions.

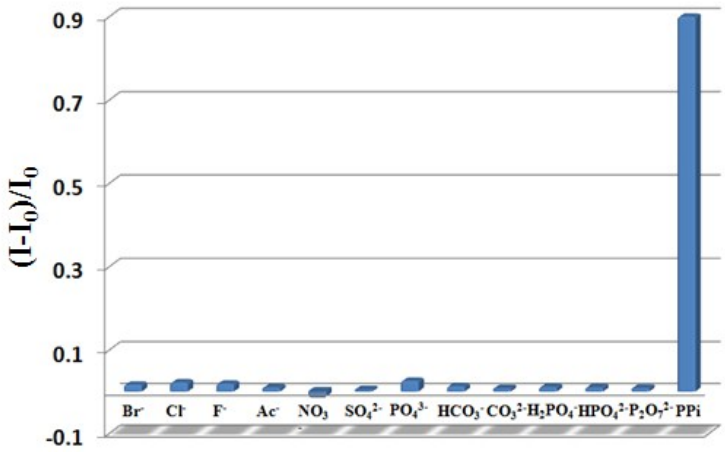

Fig. S24. Relative FL intensity $(I-I_0)/I_0$ of the sensing system in the presence of different anions. The concentration of each anion is 1000 μM. I_0 and I are the FL intensities of BNQDs-Fe^{3+} mixture in the absence and presence of PPi, respectively.

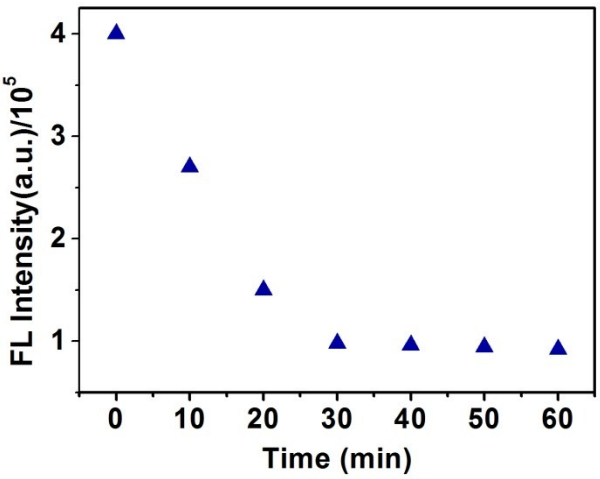

Fig. S25. Effect of incubation time between ALP and PPi on the FL intensity of the sensing system for ALP.

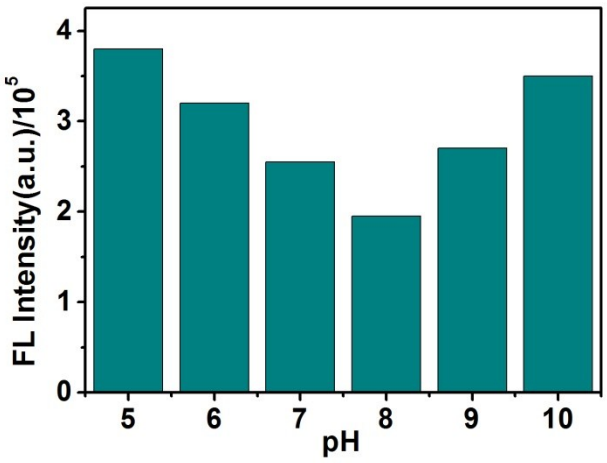

Fig. S26. Effect of pH of the background buffer on the FL intensity of the sensing system for ALP.

Table S1 The degree of fluorescence quenching of different concentrations of iron and copper ions and the degree of fluorescence recovery after addition of ppi.

Ion Concentration			5	20	50	100	200	300	400	500	600
Percentage of Fluorescence change	Percentage of quenching	Fe^{3+}	6.93 %	13.60 %	21.57 %	39.21 %	59.34 %	70.85 %	85.16 %	86.82 %	87.65 %
		Cu^{2+}	0.73 %	8.75 %	14.07 %	27.64 %	36.82 %	45.37 %	49.35 %	53.54 %	62.89 %
	Recovery Percentage	Fe^{3+}	99.75 %	99.12 %	98.32 %	98.66 %	97.48 %	96.83 %	48.48 %	35.02 %	44.37 %
		Cu^{2+}	99.58 %	99.60 %	97.68 %	98.21 %	96.52 %	99.14 %	97.57 %	95.57 %	96.87 %